

Effect of pH, L-Arginine Concentration, and Aging Time on Selenium Nanostructures

K. Prabhu,¹ K. Mohanraj,¹ S. Kannan,¹ S. Barathan,² and G. Sivakumar³

¹Department of Physics, Manonmaniam Sundaranar University, Tirunelveli, Tamil Nadu, India

²Department of Physics, Annamalai University, Annamalai Nagar, Tamil Nadu, India

³CISL, Department of Physics, Annamalai University, Annamalai Nagar, Tamil Nadu, India

Trigonal selenium nanoparticle is synthesized by precipitation method using three L-arginine concentrations and ascorbic acid and by varying aging time. In the XRD analysis, glassy nature of selenium is identified (pH \approx 2.8) and turned into hexagonal structure at $2\theta = 29.72^\circ$ (pH = 7). Average size of the particle is 29–44 nm. The FTIR result is confirmed the presence of selenium at 464 cm^{-1} and one-dimensional (1D) structural changes are detected in the FESEM photographs. Energy gap is increased from 2.24–2.72 eV up to 24 h aging time and then decreased about 2.41 eV at 48 h.

Keywords L-arginine, nanorods, nanotubes, selenium

INTRODUCTION

Selenium is an important nonmetallic element, exhibiting a large number of versatile properties, such as relatively a low melting point, high photoconductivity, a high refraction coefficient (refractive index) in devices, and nonlinear optical response, due to its characteristic structure, and it is widely used in the fields of photo electric cells, photocopiers and solar cells.^[1] During the last few years, there has been growing interest in one dimensional nanostructures owing to their novel electrical and optical properties, and potential applications in nanometer sized devices.^[2] At recently, several authors have prepared selenium nanostructures using different methods such as chemical precipitation, the sonochemical, and the hydrothermal method.^[1,3,4] The main aspects of amino acids in the synthesis of nanomaterials are to control the shape, structure of the particle and to prevent the agglomeration of nanopowder. Currently, one-dimensional (1D) selenium nanostructures

have been prepared with the assistance of amino acid such as L-cysteine and L-tyrosine.^[3,4] To know to our knowledge, the fabrication of L-arginine induced 1D selenium nanostructures is not reported elsewhere. Hence, objective of the work is to prepare 1D selenium nanostructures using SeO_2 as Se source, ascorbic acid as a reducing agent and L-arginine as a capping agent by precipitation method.

EXPERIMENTAL

In this study, the following chemicals such as selenium dioxide (SeO_2), ascorbic acid ($\text{C}_6\text{H}_8\text{O}_6$), L-arginine ($\text{C}_6\text{H}_{14}\text{N}_4\text{O}_2$), sodium hydroxide (NaOH), and ethanol ($\text{C}_2\text{H}_6\text{O}$) were used. In a typical synthesizing 500 mmol selenious acid (H_2SeO_3) was obtained by dissolve the SeO_2 in 50 mL of distilled water and stirred for 10 min. Then 200 mmol L-arginine solution was prepared by adding distilled water to the selenious acid solution. The mixture of the two solutions was again stirred for 10 min at room temperature to obtain complex solution. To obtain clear colorless solution 1000 mmol NaOH solution was added drop by drop. Finally, 300 mmol ascorbic acid solution was added dropwise slowly into the solution. Color of the solution was changed from transparent into brick red during the process. The solution was again stirred for 1 h at room temperature. After the stirring, the color of brick red color solution get changed into dark red. Then the suspension was centrifuged and thoroughly washed using distilled water and ethanol three times and obtained red selenium powder. Next, the selenium powder was allowed to recrystallize using ethanol and to age for different times by varying the aging time intervals about 3 h, 24 h, and 48 h and obtained black gray particles. Again, the samples were centrifuged and dried at room temperature. The samples were grounded using mortar and pestle for further studies. The above procedures were followed to prepare 300 and 400 mmol L-arginine concentration.

Powder X-ray diffraction (XRD) measurements were performed using PANalytical XPERT PRO diffractometer with Cu $K\alpha$ radiation ($\lambda = 1.5406\text{ \AA}$) in the range from 10° to 80° . FTIR spectra were recorded in the region $4000\text{--}400\text{ cm}^{-1}$ using Perkin-Elmer FTIR spectrometer (model RX1) with the resolution $\pm 4\text{ cm}^{-1}$. Photographs of the 1D Se nanostructures

Received 10 January 2013; accepted 27 January 2013.

The authors express sincere thanks to the UGC-SAP, New Delhi, for providing the financial support to the Department of Physics, Manonmaniam Sundaranar University, Tirunelveli, Tamil Nadu, India. Also the authors are thankful to authorities of the Manonmaniam Sundaranar University, Tirunelveli, for providing the seed money project to carry out the work.

Address correspondence to K. Mohanraj, Department of Physics, Manonmaniam Sundaranar University, Tirunelveli-627 012, Tamil Nadu, India. E-mail: kmohanraj.msu@gmail.com.

were obtained using FESEM (Curl Zeiss) technique. Optical absorption spectra of the selenium nanopowder were recorded using UV-Vis spectrophotometer (model JASCO UVIDEK-650).

RESULTS AND DISCUSSION

X-Ray Diffraction Analysis

XRD patterns of 200 mmol L-arginine assisted at different aging time of selenium is shown in Figure 1. In all the XRD patterns, there is no sharp Bragg reflection. However, a broad hump is observed between $2\theta = 15^\circ$ and 35° , which is due to amorphous selenium (a-Se) (4). The result is not changed even increases the aging time at 24 and 48 h that may be due to a low pH value (~ 2.8) of the sample.

The XRD pattern of 200 mmol L-arginine assisted with NaOH (pH ~ 6.8) at different aging time of selenium particle is shown in Figure 2 prepared the same. It is observed from the XRD patterns (Figure 2) that there is no a markable changes up to 3 h aging time. However, at 3 h, a diffraction peak emerging at $2\theta = 29.72^\circ$, which is corresponds to the (1 0 1) plane which is due to the t-Se and it is predominantly developed along the unique [0 0 1] direction. It is also parallel to the helical chains of

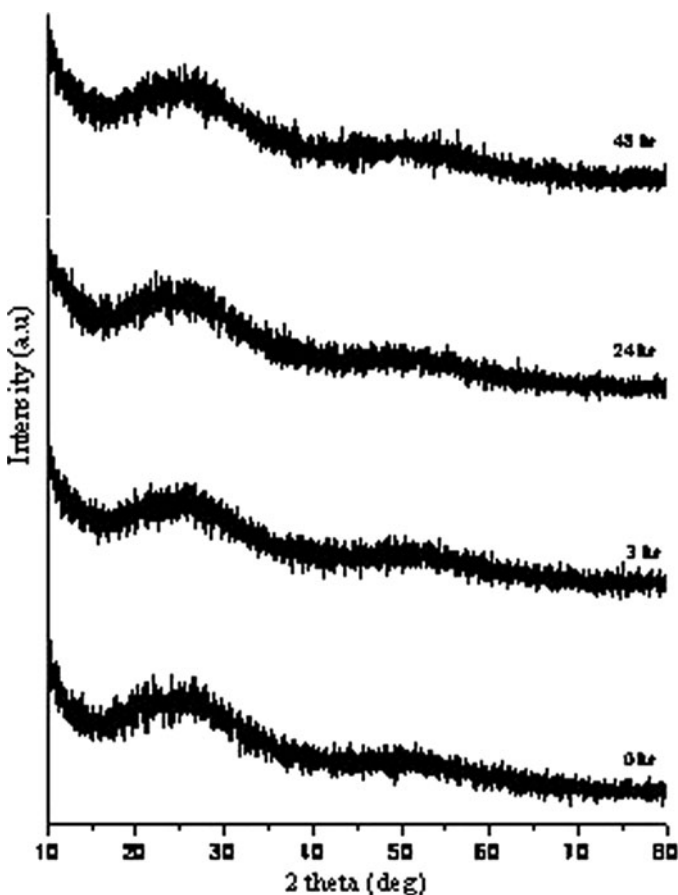


FIG. 1. XRD patterns of selenium nanopowders using 0.2M L-arginine without NaOH at different aging time.

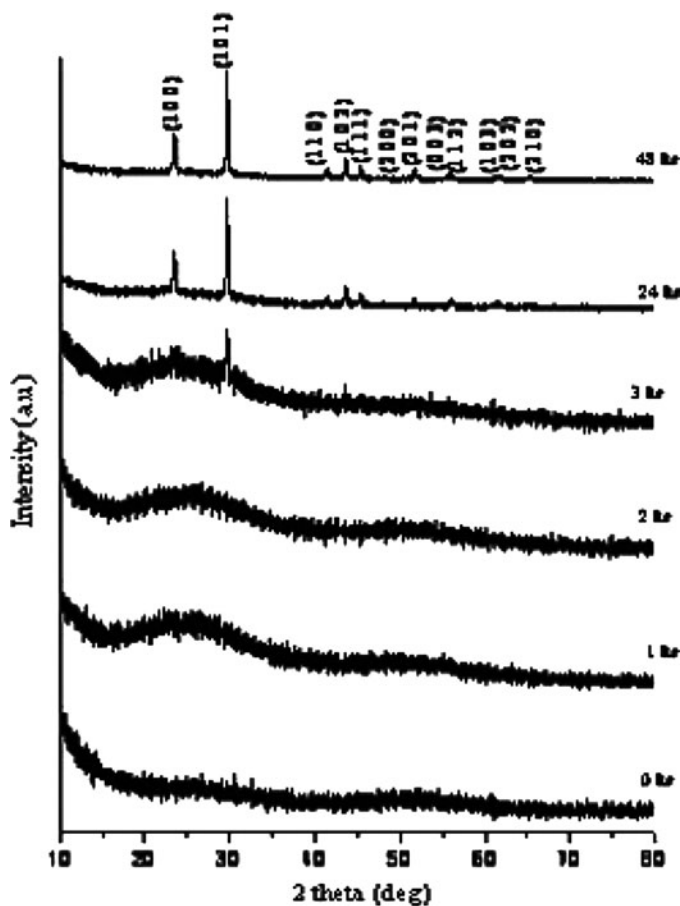


FIG. 2. XRD patterns of selenium nanopowders using 0.2M L-arginine with NaOH at different aging time.

Se atoms or the c -axis. This suggests that transformation of a-Se into t-Se takes place from 3 h onward. At higher aging time (24 and 48 h), the characteristic peak (29.72°) get sharp and strong intensity. Also some peaks with medium intensity peaks observed at 23.56° , 41.33° , 43.64° , 45.40° , 48.17° , 51.68° , 55.57° , 56.12° , 61.20° , 61.69° , and 65.31° , which are corresponds to (1 0 0), (1 1 0), (1 0 2), (1 1 1), (2 0 0), (2 0 1), (0 0 3), (1 1 2), (1 0 3), (2 0 2), and (2 1 0) planes. The characteristic peaks are indexed to the hexagonal phase of selenium (JCPDS Card no: 06-0362) and the results are in agreement with the early report.^[5] In addition to this no other impurities are seen in the XRD patterns, that is confirmed pure hexagonal selenium (t-Se).

XRD patterns of 300 and 400 mmol L-arginine assisted with NaOH (pH ~ 6.8) at different aging time of selenium is shown in Figures 3 and 4, respectively. In absence of aging (Figure 3), the reaction products are amorphous. However, the characteristics peaks are emerging from 1 h that is rapid transformation of a-Se into t-Se when compared to 200 mmol L-arginine with NaOH. As time proceeds, unstable selenium (a-Se) is grown into metastable state^[6] and attained more stable (t-Se) at 24 and 48 h. In addition to this, a medium intensity peak is observed at 38.46° which is confirmed the presence of sodium hydrogen

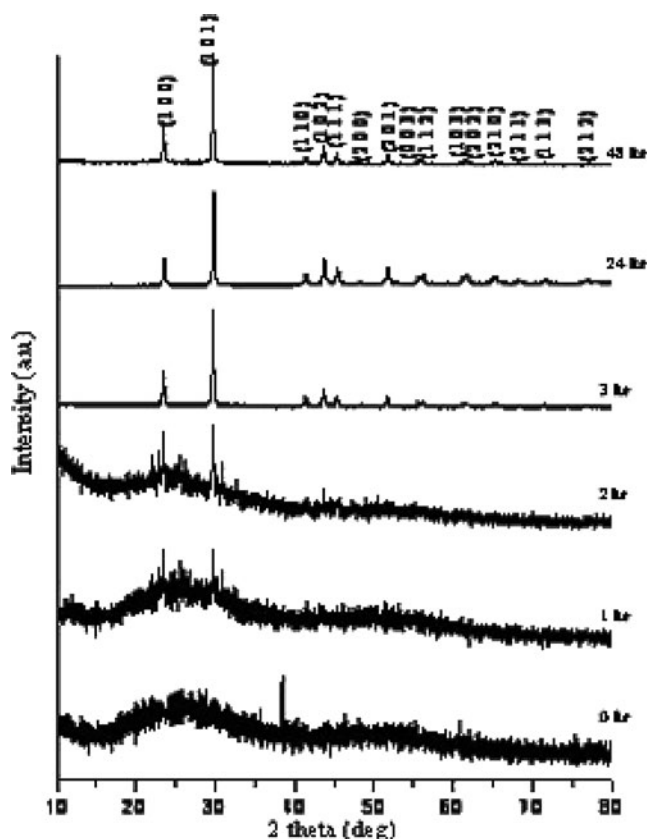
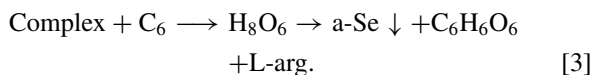
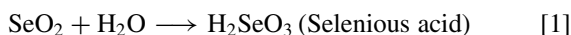


FIG. 3. XRD patterns of selenium nanopowders using 0.3M L-arginine with NaOH at different aging time.

selenide (NaHSeO₄) impurity (JCPDS card No: 510150). It may be formed during washing.

Figure 4 shows the transformation of a-Se into t-Se is started after 3 h aging that exhibit retardation reaction than 300 and 200 mmol L-arginine with NaOH. The transformation of a-Se into t-Se is compared in three concentrations that is marked at 3 h for 200 mmol, 2 h for 300 mmol, and 24 h for 400 mmol L-arginine with NaOH. The 300 mmol L-arginine is rapid transformation among the three concentrations. The following three equations can be explained the formation of Se.



The peak at the lower angle is more meaningful for the calculation of particle size. The average crystallite size of selenium is calculated using the Scherrer equation:

$$D = K\lambda / \beta \cos\theta \quad [4]$$

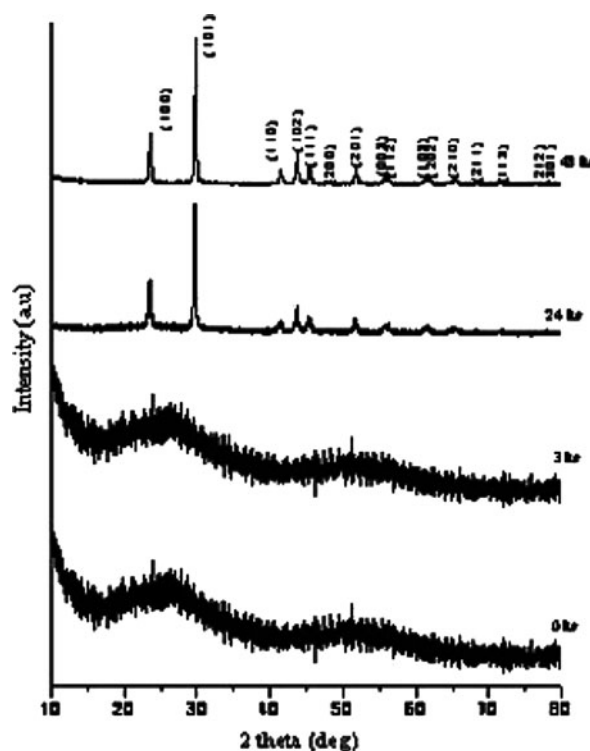


FIG. 4. XRD patterns of selenium nanopowders using 0.4M L-arginine with NaOH at different aging time.

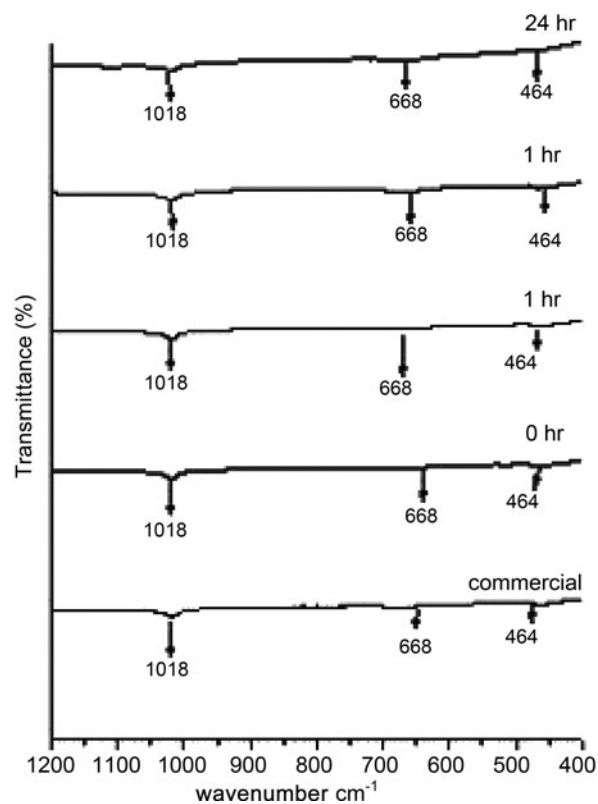


FIG. 5. FTIR spectra of commercial and synthesized selenium particles.

where D is the grain size, K is the constant taken to 0.9, λ is the wavelength of the X-ray radiation, β is the full width at half maximum, and θ is the angle of diffraction. From the previous relation, the crystallite size of the selenium particles is found in the range about 44–39 nm for 200 mmol, 32–29 nm for 300 mmol, and 39–37 nm for 400 mmol L-arginine. It is noticed that crystallite size decreased with increasing aging time.

FTIR Analysis

The FTIR spectra of selenium particles are shown in Figure 5. A peak with weak intensity in the commercial selenium is detected at 464 cm^{-1} , which is due to selenium. Also, a band with weak intensity at 668 cm^{-1} is due to Se-O bending vibration of selenious acid (H_2SeO_3) and a band at 1018 cm^{-1} is due to SeO_2 . These results are with the earlier reports.^[7–9] The observed results are prove in synthesized selenium.

Microstructural Analysis

Figure 6 shows the FESEM images of 300 mmol L-arginine with NaOH of selenium nanopowders. In Figure 6, a large number of needle like selenium products are acicular and reticular structure. Although some spherical particles are beneath among the needles that are approximately less than 100 nm. Average length of the needles are less than $1\ \mu\text{m}$ and the needles are grown much and formed nanosize rods at 3 h aging. Average

diameter of the needles are less than 50–60 nm. At 3 h aging the spherical particle are not shown in the micrograph that is attributed to crystallization process started. This result is consistent with the earlier report^[10] and also supported to the XRD results. In 24 h aged FESEM photograph (Figure 6), distinct nanorods of selenium are dispersed on the surface. Figure 7 shows the average diameter of the rods is about 30–50 nm and length up to several micrometers. Formation of selenium rod is coinciding well with the earlier report on fabrication of selenium rods using different solvents.^[11] A 48 h aging time (Figure 6), the selenium nanorods the average diameter of the tube is found about 70–80 nm and length up to several micrometers.

Optical Analysis

The optical absorption spectra of 300 mmol L-arginine assisted selenium nanopowder. In the absorption spectra optical absorptions percentage increase with increasing aging time. There are three absorption peaks shown in the spectrum at 500, 415, and 325 nm and then the peaks gradually decreased in the visible region. It indicates that the transformation of a-Se to t-Se phase and the result is in agreement with the earlier reports on t-Se nanowires by sonication of a-Se in ethanol.^[12] It is worth noting that the absorption peaks appear above 530 nm can be solely attributed to interchain interactions perpendicular to the

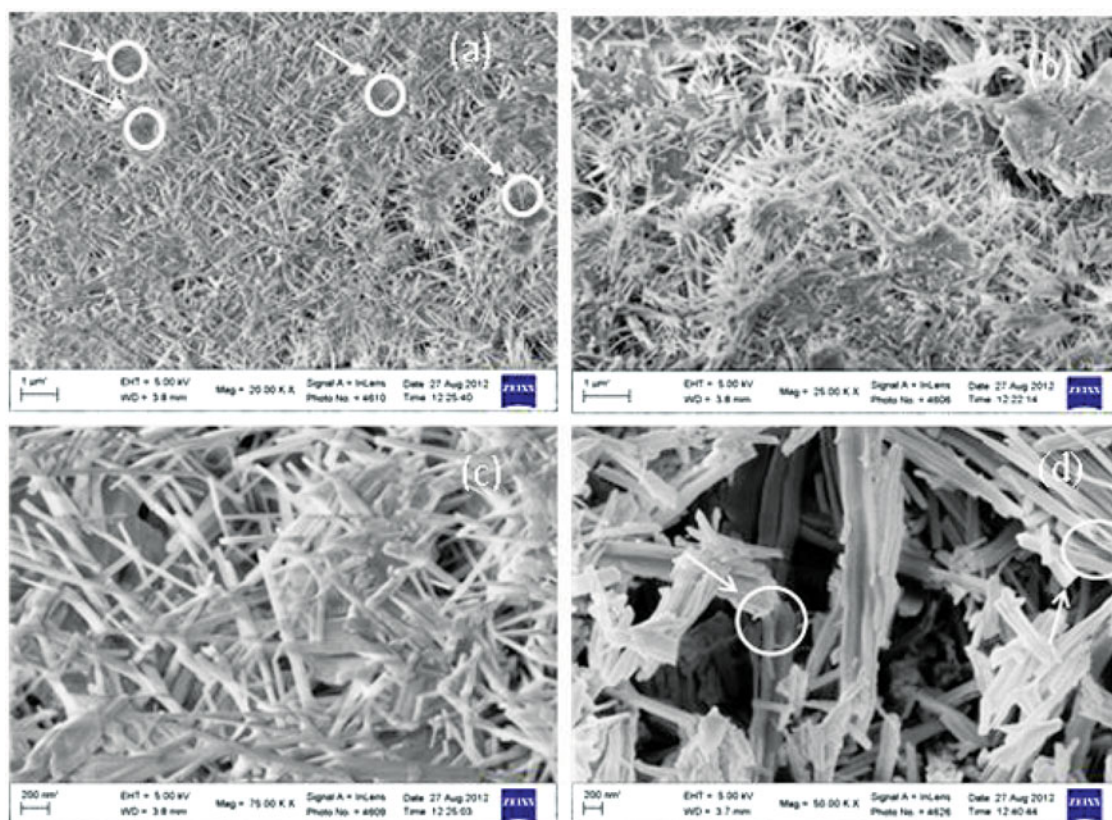


FIG. 6. FESEM images of selenium nanostructures at different aging (a) 1 h, (b) 3 h, (c) 24 h, and (d) 48 h. (color figure available online).

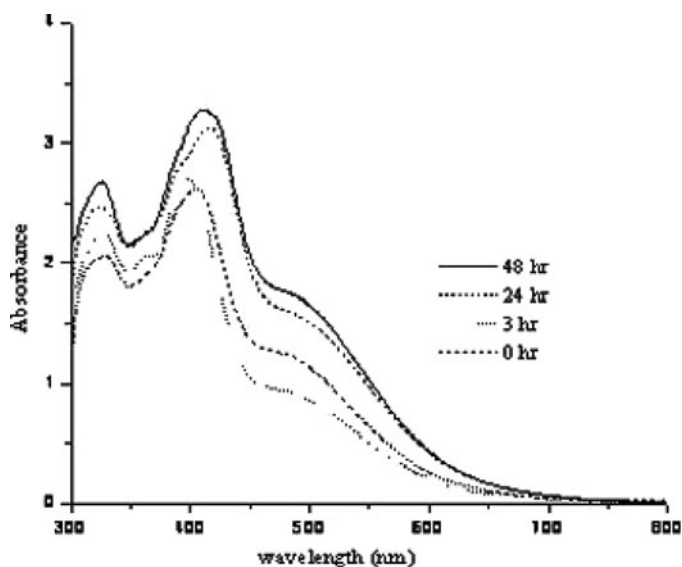


FIG. 7. UV-visible spectra of selenium nanopowders using 0.3M L-arginine with NaOH.

c axis within a given *t*-Se crystal, hence the position of the low-energy peak at high wavelength may provide instructive information for the interchain interactions as well as the degree of crystal perfection. The characteristic absorption peaks within the range between 325 and 425 nm can be regarded as an excitonic peak for Se nanostructure and proves the existence of Se nanopowder. The result is in agreement with the earlier report.^[13]

The fundamental absorption, which corresponds to electron excitation from the valence band to conduction band, can be used to determine the value of the optical band gap. The relation between the absorption coefficient (α) and incident photon energy ($h\nu$) can be written as

$$(\alpha h\nu) = A (h\nu - E_g)^n \quad [5]$$

where A is constant, E_g is the band gap of the material, and exponent n depends on the type of transition. Here the transitions are direct so we can take $n = 1/2$.

The optical band gaps (Figure 8) were calculated by extrapolating the straight line portion of $(\alpha h\nu)^2$ versus the $h\nu$ graph for selenium nanopowder using 300 mmol L-arginine.

From the previous relation (Eq. 5), the optical band gap energy is increased from 2.24–2.72 eV for 24 h and then decreased about 2.41 eV for 48 h. However, the observed band gap values are higher than that of bulk Se (1.7 eV), which is due to the quantum confinement effect.^[13]

In this conversion process, when the *a*-Se was dispersed in ethanol, and the *a*-Se gradually dissolved to form a metastable solution, and then the selenium atoms recrystallized on the *t*-Se in ethanol. At this time, the anisotropic characteristic of the *t*-Se provided a natural template to guide the growth of Se atoms

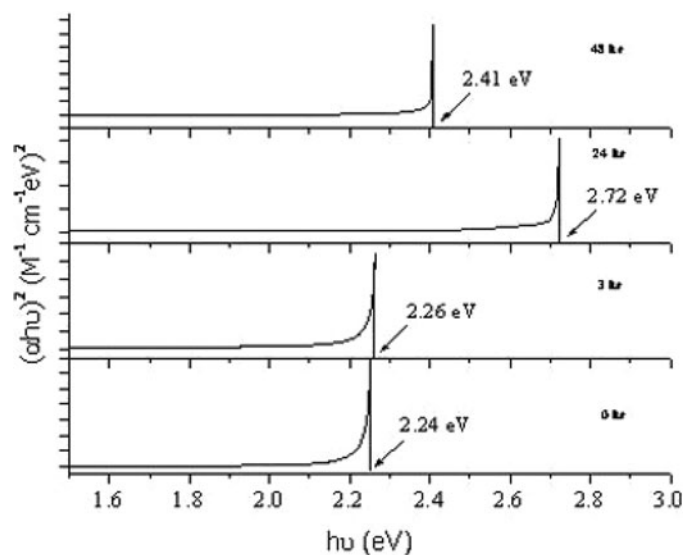


FIG. 8. Band gap energy of selenium nanopowder using 0.3M L-arginine with NaOH.

along one particular axis (*c*-axis) and thus the products turned out to be nanorods and nanotubes. The solvent in which the *a*-Se is dispersed plays an important role in the Se nanorods growth in the conversion. If water was used instead of ethanol, only massive Se products were found instead of *t*-Se nanorods and thus an appropriate solvent in which the solubility *a*-Se is larger than that of *t*-Se is important to ensure conversion of the initial *a*-Se to the *t*-Se nanorods.

CONCLUSIONS

The following results are drawn from the experimental studies.

- The XRD analysis confirmed the hexagonal phases of selenium particles and that conversion of *a*-Se into *t*-Se at 3 h for 200 mmol, 2 h for 300 mmol and 24 h for 400 mmol L-arginine with NaOH among the three concentrations. The 300 mmol L-arginine is rapid conversion with respect to aging time. The average size of selenium particles are found in the range 44–29 nm.
- The FTIR results are confirmed the characteristics of Se-O vibrations in both commercial and synthesized selenium at 464 cm^{-1} , 668 cm^{-1} , and 1018 cm^{-1} .
- 1D nanostructural changes are visually seen in the FE-SEM micrographs. Average diameter of the nanorods and nanotubes are found to be less than 30–80 nm.
- In the UV-Visible analysis, optical absorption increase with increase the aging time and there are three maximum absorption peaks at 500, 415, and 325 nm. The band gap energy is increased from 2.24–2.72 eV for without aging and up to 24 h and then decreased about 2.41 eV for 48 h. It is concluded from the above

experimental reports that, the t-Se phase having higher optical absorptions characteristics in the visible region. Hence, the material can be used for fabrication of nanoscale optoelectronic devices.

REFERENCES

1. Ma, J.; Liu, X.; Wu, Y.; Peng, P.; Zheng, W. Controlled synthesis of selenium of different morphologies at room temperature. *Cryst. Res. Technol.* **2008**, *43*, 1052–1056.
2. Chen, H.; Shin, D.-W.; Nam, J.-G.; Kwon, K.-W.; Yoo, J.B. Selenium nanowires and nanotubes synthesized via a facile template-free solution method. *Mater. Res. Bull.* **2010**, *45*, 699–704.
3. Mondal, K.; Roy, P.; Srivastava, S.K. Facile biomolecule-assisted hydrothermal synthesis of trigonal selenium microrods. *Cryst. Growth Des.* **2008**, *8*, 1580–1584.
4. Wang, X.; Zhang, W.; Shen, Y.; Huang, L. Facile, one-step controlled synthesis of Se nanocrystals in the presence of L-tyrosine. *Mater. Sci. Eng. B* **2011**, *176*, 1093–1098.
5. Zhu, W.; Xu, H.; Wang, W.; Shi, J. Controlled synthesis of trigonal Selenium nanowires via a facile solution route. *Appl. Phys. A Mater. Sci. Proc.* **2006**, *83*, 281–284.
6. Znan, B.; Ye, X.; Dai, W.; Hou, W.; Zuo, F.; Xie, Y. Biomolecule-assisted synthesis of single-crystalline selenium nanowires and nanoribbons via a novel flake-cracking mechanism. *Nanotechnol.* **2006**, *17*, 385–390.
7. Ma, Y.; Qi, L.; Shen, W.; Ma, J. Selective synthesis of single-crystalline selenium nanobelts and nanowires in micellar solutions of nonionic surfactants. *Langmuir* **2005**, *21*, 6161–6164.
8. Li, X.; Li, Y.; Li, S.; Zhou, W.; Chu, H.; Chen, W.; Li, I.L.; Tang, Z. Single crystalline trigonal selenium nanotubes and nanowire synthesized by sonochemical process. *Cryst. Growth Des.* **2005**, *5*, 911–916.
9. Chen, Y.-W.; Li, L.; D’Ulivo, A.; Belzile, N. Extraction and determination of elemental selenium in sediments—a comparative study. *Anal. Chim. Acta* **2006**, *577*, 126–133.
10. Xi, G.; Xiong, K.; Zhao, Q.; Zhank, R.; Zhang, H.; Qian, Y. Nucleation–dissolution–recrystallization: a growth mechanism for t-selenium nanotubes. *Cryst. Growth Des.* **2006**, *6*, 577–582.
11. Patil, Y.; Kanna, P.K. Fabrication of selenium rods by solution method. *Synth. React. Inorg. Met.-Org. Nano-Met. Chem.* **2008**, *38*, 518–523.
12. Gates, B.; Mayers, B.; Grossman, A.; Xia, Y. A sonochemical approach to the synthesis of crystalline selenium nanowires in solutions and on solid supports. *Adv. Mater.* **2002**, *14*, 1749–1752.
13. Mekta, S.K.; Chaudhary, S.; Kumar, S.; Bhasin, K.K.; Torigoe, K.; Sakai, H.; Abe, M. Surfactant assisted synthesis and spectroscopic characterization of selenium nanoparticles in ambient conditions. *Nanotechnol.* **2008**, *19*, 295601–295611.

Copyright of Synthesis & Reactivity in Inorganic, Metal-Organic, & Nano-Metal Chemistry is the property of Taylor & Francis Ltd and its content may not be copied or emailed to multiple sites or posted to a listserv without the copyright holder's express written permission. However, users may print, download, or email articles for individual use.